

## Field observations, Petrography and microstructures study of Jebale Barez Plutonic complex (East - North East Jiroft)

Jamal Rasouli<sup>1\*</sup>, Mansor Ghorbani<sup>1</sup>, Vahid Ahadnejad<sup>2</sup>

1- Department of Geology, Faculty of geosciences, Shahid Beheshti University, Tehran, Iran.

2- Department of Geology, Payame Noor University, P.O Box 19395-3697, Tehran, Iran.

\* Corresponding Author: Jamal.rasouli1362@gmail.com

Received: 01 February 2014 / Accepted: 22 July 2014 / Published online: 28 July 2014

### Abstract

Jebale Barez Plutonic Complex Is composed of granitoid Intrusive Bodies and Is located In the East - North East Jiroft and southeastern province of Kerman on The lengths of the 57° 45' east to 58° 00' and Northern latitudes 28° 30' to 29° 00'. Plutonic Complex composed of granodiorite, quartzdiorite, Monzogranite and Porphyritic granite. The microstructures observed in thin sections from about 200 samples in this study were grouped into three types: (i) magmatic microstructures; (ii) submagmatic microstructures and (iii) Mylonitic microstructures. Magmatic microstructures and submagmatic microstructures located in the central of Mijan and less than in the central of Hishin and Korour area but Mylonitic microstructures observed in all of rims Jebale Barez Plutonic Complex. Field observations, Major structural and morphologic elements suggested that Mijan area is old caldera and Evidence suggested that Magma implemented Sill form in the Jebale Barez Plutonic Complex. Therefore it is assumed that the whole JBPC is located in shear zone. Mijan Old Caldera is feeder zone and magma has been intrusion. Magma has been percolated through Mijan caldera and emplacement Forms of Sill along the shear zone during various periods.

**Keywords:** Granite, Microstructures, Jebale Barez, Urumieh-Dokhtar magmatic belt.

### 1-Introduction

From their first use in the 19th century, thin sections of rocks have been an important source of information for geologists (Passchier, 1982a). However, did not treat microscopic aspects of structures, while petrologists would describe microscopic structures as, for example, lepidoblastic or nematoblastic without paying much attention to kinematic and dynamic implications. During the last decades, however, structural geologists learned to profit from the wealth of data that can be obtained from the geometry of structures studied in thin section, and metamorphic petrologists have appreciated the relation of structural evolution on the thin section scale and metamorphic processes (Vernon, 1993). Deformed rocks are one of the

few direct sources of information available for the reconstruction of tectonic evolution. Nevertheless, observations on the geometry of structures in deformed rocks should be used with care; they are the end product of an often complex evolution and we can only hope to reconstruct this evolution if we correctly interpret the end stage (Vernon, 1989). Observations on the microstructure or fabric of a rock specifically in thin section can be used in two major fields. They can be applied to thematic studies, to understand mechanisms of rock deformation and metamorphism; or they can be used to reconstruct the structural and metamorphic history of a volume of rock. Thin section studies are mostly in the latter field. Because such thin section studies can serve to reconstruct tectonic evolution (Passchier,

1982a), we use the term microtectonics. Fortunately for the geologist, who relies on structures and mineral assemblages in deformed rocks as a source of information, this is almost never the case (Vernon, 2000). In most deformed rocks, structures with different style and orientation and minerals, which represent different metamorphic grades, overprint each other. This means that equilibrium is generally not attained at each stage: mineral assemblages representative of different metamorphic conditions may be 'frozen in' at different stages during burial and uplift. With overprint we mean that structures or mineral assemblages are superposed on each other and must therefore differ in age; this may be visible through crosscutting relations, overgrowth, or even differences in deformation intensity (Passchier, 1982b). For all overprinting relations it is necessary to determine whether they could have formed during a single phase of deformation under similar metamorphic conditions. The following criteria may help to determine whether overprinting relations correspond to separate deformation phases: a) two overprinting structures composed of different mineral assemblages that represent a gap in metamorphic grade must belong to different deformation phases. b) Foliations that overprint each other commonly represent deformation phases on thin section but exceptions such as oblique fabrics and shear band cleavages exist. c) Overprinting folds with oblique axial surfaces represent different deformation phases. Care should be taken with refolded folds with parallel axes (Type and Ramsay, 1967), especially in the case of isoclinal folds since these may form during a single deformation phase. d) Shortened boudins are commonly formed by overprinting of two deformation phases (Passchier, 2002). e) Some structures preserved in porphyroblasts represent separate deformation phases. f) Intrusive veins or dykes can be important to separate phases of deformation and their associated foliations. Microstructures provide essential information in a broad range of studies

in deformed igneous and metamorphic rocks. Igneous rocks are classified according to their source rock type, structure; microstructure and mineral composition (see more in the principles of the IUGS scheme for Classification of Igneous Rocks). Correlating granite emplacement and deformation with regional tectonic events is a challenge because granitic rocks do not always develop mesoscopic scale deformation fabrics. Microstructural studies of granites can help to identify magmatic or solid-state deformation fabrics (E.G. Simpson 1985; Paterson *et al.*, 1989; Bouchez *et al.*, 1992), on the basis of which granite can be interpreted as deformed. In itself, this cannot lead to infer the relationship between a regional deformation event and development of a fabric in granite. Additional information is required, in particular on the orientation and spatial distribution of these fabrics and their relationship with host rocks of the granite pluton in question (Mainprice *et al.*, 2003). Mineral composition is a parameter that reflects the proportions of the individual minerals within the rock. Rock structure represents all of the macroscopically visible characteristics such as foliation, lineation, folding, and faulting (Spry, 1969; McLaren *et al.*, 2001; Bucher and Frey, 1994). Microstructure comprises the geometrical parameters of rock-forming minerals such as grain size, grain shape, and spatial arrangement of minerals visible in micro-scale (Vernon, 2000). Most of the parameters mentioned above are commonly described qualitatively, employing polarizing microscopy. The combination of polarising microscopy along with image analysis makes it possible to determine the mineral composition, as well as the microstructural parameters quantitatively (e.g., Heilbronner, 2000; Trčková *et al.*, 2008), which increases the objectivity and accuracy of the microscopic description. In this study, we employed the information from field-based and laboratory studies on macro and microstructure analyses, respectively. Field observations and petrofabric studies of well-exposed Jebale Barez

Plutonic complex (JBPC) could provide evidences for their formation and emplacement processes to depict regional crust evolution. We are currently working on microstructural development of JBPC that deform as they are

crystallizing. In addition, we are evaluating microstructures in igneous rocks JBPC in order to better understand the relations between deformation and magmatism.



Figure 1) Field photographs showing characteristics of Jebale Barez Plutonic complex (a) Outline of lithological units in the study area, (b) Porphyritic granite in the Mijan area, (c) The Second Unit Intrusive rocks In the study area, (d) The third Unit Intrusive rocks In the study area, (e) Despite fragmentation and fracture in rocks, (f) Enclaves with fine-grained in granite.

## 2– Geological setting and field observations

The Iranian realm has passed various geological events since early Precambrian. Because those events were not uniform, variety in magmatism and metamorphism, different style in structural geology and deformations, general trends and sedimentary basins led to a variable structural pattern on this plateau. Looking at the geological situation of Iran and concerning the structures and different formations it is revealed that different parts of this country got its particular aspects through time distinguishing them as different zones. Regarding that, the geologists have divided the Iranian plateau in some structural-sedimentary zones with special characteristics. Using the structural division by Nabavi (1977) the study area is located to the southern parts of Central Iran zone on the Urumieh-Dokhtar magmatic belt (UDMA) which is parallel to Sanandaj-Sirjan Zone. Central Iran which is as a large triangle zone in the centre of Iran is one of the most complicated zones of Iran. In fact it could be considered as a part of oldest continent in Iran which endured lots of geological events. Because its width and variety and regarding to structural features and different rock types that is divided in different parts (Darvishzadeh, 2005).

Urumieh-Dokhtar magmatic belt (UDMA) is mainly a magmatic belt with northwest-southeast direction. This belt starts from Western Europe in Serbia and stretches out to the east into Anatolia and then into Iran via Turkey border. This belt with some 1500 km length and 100 km width is extended from Sahand to the Bazman and then enters in Pakistan. Magmatism in the UDMA started since Ypresian in Eocene (Emami, 1981) with a highest activity in the Middle Eocene. The magmatic nature in this zone is mainly of calc-alkaline and in minority of alkaline. Some magmatic characteristics of UDMA could be summarized as follow (Ghorbani, 2013): a)

Magmatism continued up to Quaternary in the UDMA. The magmatic activities have some picks in the Middle Eocene, Upper Eocene, Lower Oligocene, Upper Oligocene, Lower Miocene and Mio-Pliocene. b) The petrography of magmatic rocks in the UDMA is variable ranging from basalt to rhyolite but most of them consist of andesites. c) Lots of plutons from diorite to granite with majority in tonalite-granodiorite intruded the volcanic rocks. They are mainly of Upper Eocene-Lower Oligocene in age. From tectonic point of view this zone is situated in parallel trend with Sanandaj-Sirjan Zone, cutting the Nain-Baft belt so that, some ophiolitic bands are exposed to the southern parts of that. This feature is very important in terms of the metallogeny. Some petrologists (Amidi *et al.*, 1977; Sabzehei, 1994; Emami, 1981; Caillet *et al.*, 1978) believe that the tectonic setting of UDMA belongs to continental rift, and on the other hand tectonic experts believe that its tectonic setting is associated with subduction zone (Aftabi and Atapour, 2000; Moine-Vaziri, 1985; Berberian and Berberian, 1981; Takin, 1972). magmatic activities exist as both volcanic and intrusive rocks. The magmatic rocks in this area followed the same trend of the main structure trending NW-SE. in general the whole magmatic activities could be categorized in four events (Ghorbani, 2013): The first phase has been of Jurassic age which is the oldest event in this region. That is composed of volcanic such as basalts and intrusives like granite, garnodiorite and diorite cropping out to the southwestern parts of the study area. They started from Early Jurassic continued up to Late Jurassic. The beginning of magmatism was in submarine volcanism as spilites/basalts and later it changed to granitoids and diorites. The latter one is less important. To the west of Delfard fault there is an intrusive body of Jurassic according to published geological map but the geologists of this study that should be the same age of Jebale Barez intrusive bodies.

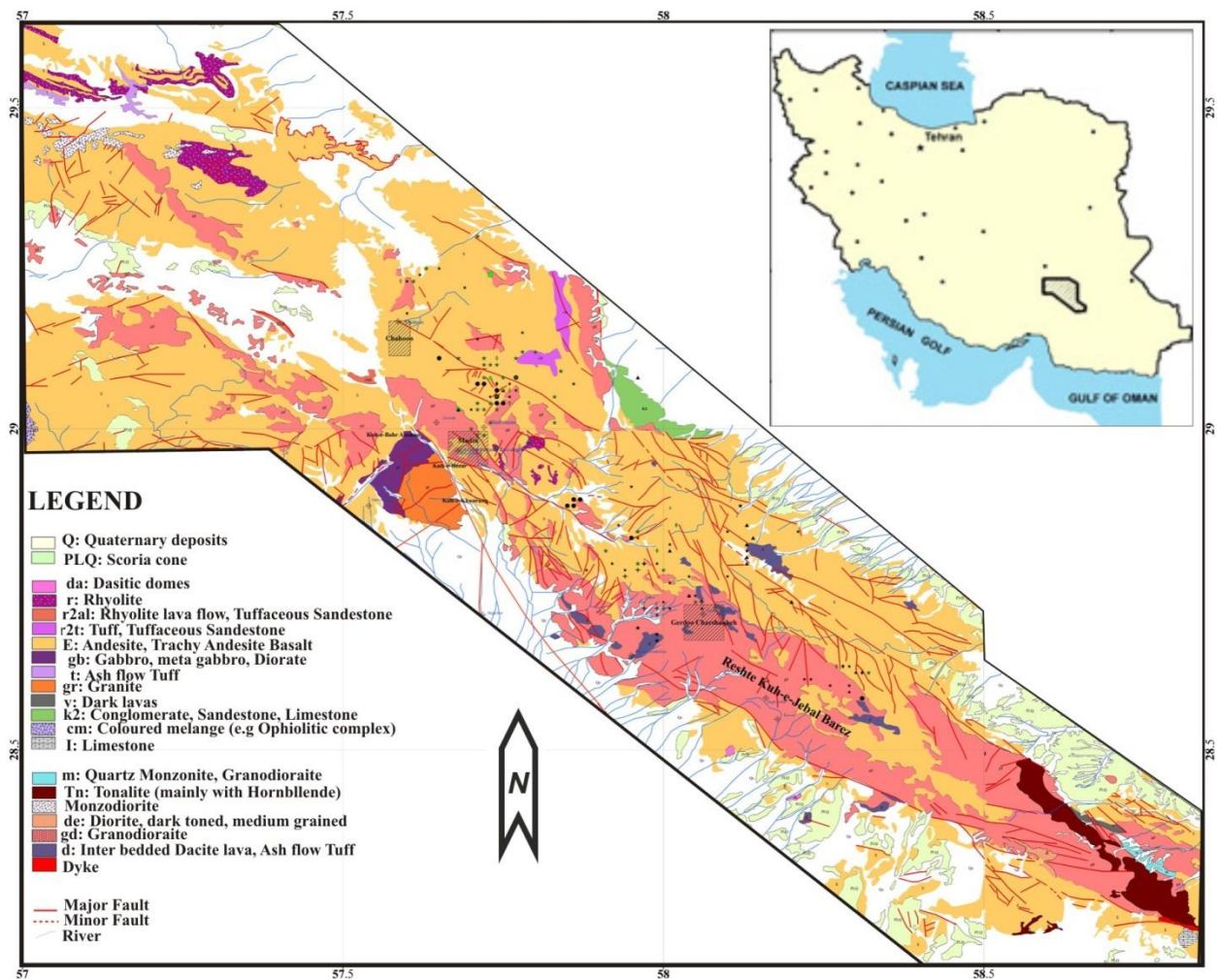


Figure 2) Geological map of the study area.

The second phase goes back to Eocene with a considerable development in the area. That is mainly of extrusive and consists of rhyolite, porphyry rhyodacite, porphyry dacite, andesite and andesibasalt. They are seen throughout the region. The third one is of Oligo-Miocene age. This phase occurred as intrusive in this area and the small stocks led to copper porphyry deposits in the Kerman region. The composition is of porphyry granodiorites to porphyry thakite and porphyry diorites (Fig. 1b). They generally intruded the Eocene volcanic rocks. The latest phase in the study area is of Quaternary basalts which are very rare. Figure 2 shows a simplified geological map of the Jebale Barez Plutonic complex (JBPC). The formation of this complex was followed by the development of volcanic complexes during the Eocene (Razak complex) and Oligocene (Hezar complex), which consist of trachybasalt, andesite, trachyandesite,

andesite–basalt, and acidic tuff (Dimitrijevic, 1973; Hassanzadeh, 1993; Shafiei *et al.*, 2009). The Oligocene–iocene intrusive rocks in JBPC were emplaced into the volcanic rocks. These rocks consist of granodiorite, quartzdiorite, granite and monzogranite and also these rocks includes abundant of rounded and ellipsoid Magmatic enclaves composed of quartz diorite, monzodiorite and quartz monzodiorite (Fig. 1f).

JBPC possesses characteristics (Fig. 3): a) Its lithology varies from diorite to granite, b) This complex intruded within thick volcanic-pyroclastic rocks of Eocene, c) Metamorphic rims sometimes observed at the contacts between the complex and Eocene units, d) Intrusive bodies (first penetration phase) of JBPC includes consecutive retarder bodies with more similar compositions. These retarder bodies which intruded within JBPC include: a) Light-colored granite–alkali granite bodies

specially at Mijan Area (second intrusive phase at Mijan Area), b) Variably distributed Diorite bodies that usually observed at fault zones [second phase at JBPC (Fig. 1c)], c) Leucocratic porphyry acid bodies with alkali granite, alkali syeno-granite to quartz syenite compositions and different petrographies [third intrusive

phase (Fig. 1d)]. They are usually leucocratic-hololeucocratic and light-colored with low mafic minerals (or their mafic minerals may be removed during alteration). Intrusive body at JBPC include: Rigan, Korour, Bagh-e-Golan, Darreh Hamzeh, Mijan, Tenaroiieh, Madian, Zavarak, Hishin and Gerdo Charshanbeh.

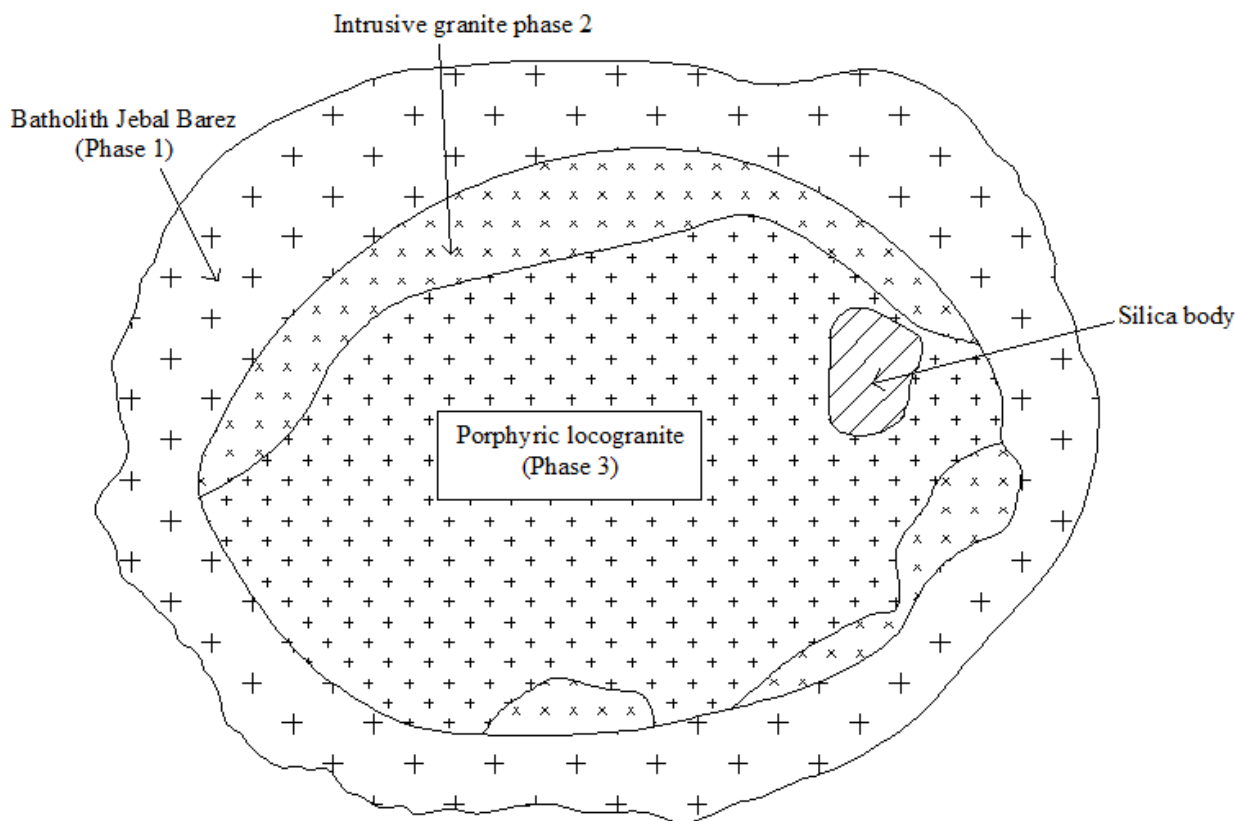


Figure 3) Schematic view of magmatism in Jebale Barez Plutonic complex (JBPC) (without scale).

The geochemical variation diagrams of major oxides, the continuous spectrum of rock compositions has been carried out which indicates the crystallization of magmatic differentiation and extensive appendices. The magma nature of these rocks is sub-alkaline-calc-alkaline, which in SiO<sub>2</sub>-K<sub>2</sub>O plot they fall into calc-alkaline series with high potassium. Field observations, petrographic and geochemical studies suggest that the rocks in this area have granitoides I type. Studying the geochemical diagrams of the rocks in the studied area indicates that these rocks have been formed in active continental margin tectonic setting. Most of the volcanic arc granites (VAG) are of "pre-collision" and "syn-collision" types. Based on The location of Urmia-Dokhtar

magmatic belt seems The rocks of this region There came to subducted oceanic crust Neotethyan beneath continental crust of central Iran.

This area tectonically has been active since Cretaceous to Pleistocene (Ghorbani, 2013). Its evidence could be seen as volcanic activities and intrusions which all happened in continuation of subduction of oceanic slab below continental crust (Ghorbani, 2013). Outpouring of such thick volume of lavas and pyroclastics during Eocene, and subsequent frequent foldings, uplifting and weathering/erosion are all signs of early Alpine orogeny. The formation of marine shallow sediments in Oligocene indicates the lowest activities during this time (Darvishzadeh, 2005).

In the early Miocene, Arabian plate collided with Central Iran leading to intensification of volcanism accompanied with uplifting and formation of thick conglomerates. In parallel, the stratovolcanoes were more active leading to emplacement of batholites and intrusions. During the late Miocene, some stocks, plagues, sills and dykes formed around the main intrusive bodies. The presence of unreformed beds at the Late Miocene indicates a quieter period which followed by uplifting, weathering, and sedimentation in Pliocene. The presence of a thick basaltic horizon overlying those conglomerates indicates the resumption of volcanism until Pleistocene (Darvishzadeh, 2005). As the mentioned tectonic activities associated with Zagros subduction, the faulting followed the main trend of northwest-southeast which likely were active through the Tertiary. Those faults locating to the border of batholites were probably formed due to the emplacement of intrusions in the Late Oligocene-Early

Miocene (Fig. 1e). The faults trending north-south which dislocated those border faults are probably implying some sort of activities along the Oman line and or the continuation of Nayband system through the Late Miocene. The final activities of faulting could be associated with an important fault system trending northeast-southwest likely separated from Kahurak fault located to the east of Lut block. It seems these faults changed their trends along the border of Central Iran resistant block due to the orogenic activities (Ghorbani, 2013).

### 3–Petrography

Detailed mapping of the JBPC (Fig. 2) distinguished four main rock types, hereafter referred to As the granodioritic unit, quartz-dioritic unit, monzogranitic unit and Porphyritic granite unit. More than 200 samples of all rocks facies were obtained for detailed petrographic and microstructural analysis.

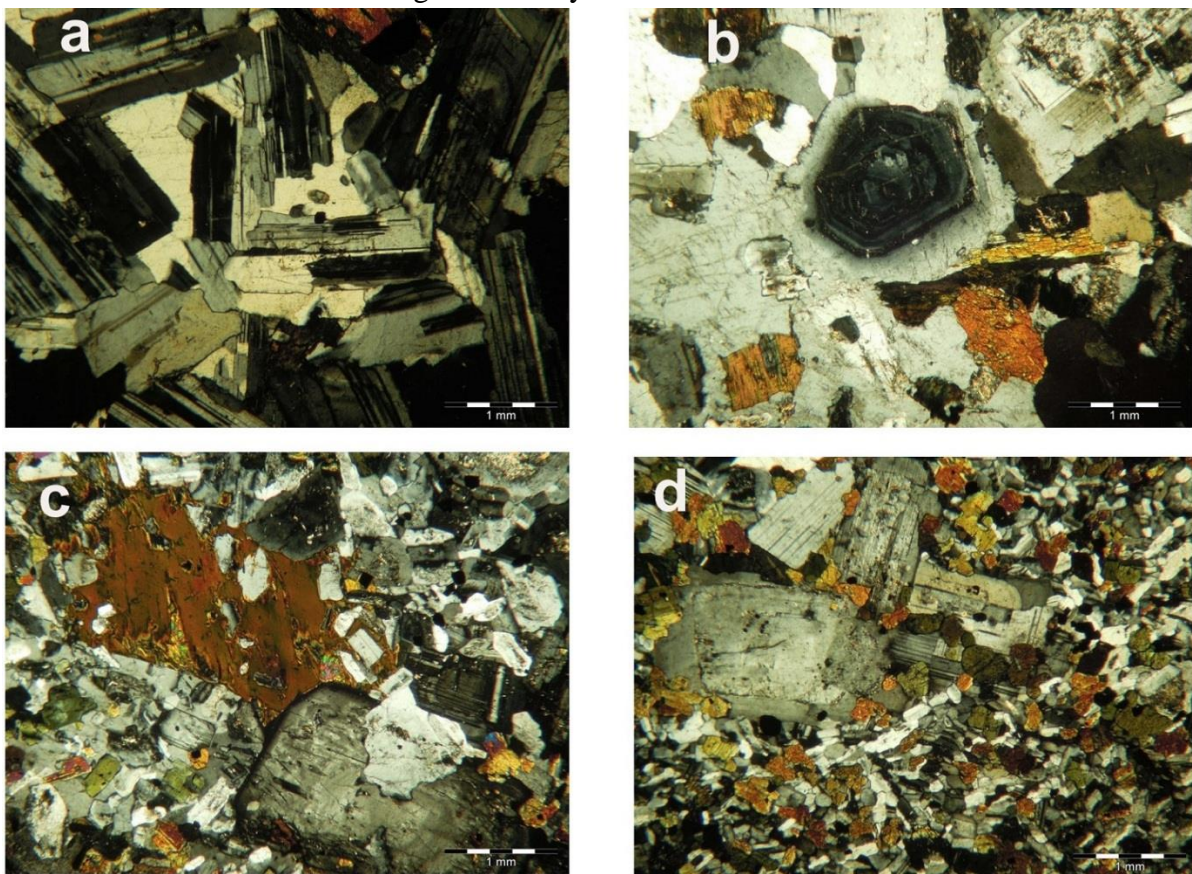


Figure 4) Microphotographs of representative samples (crossed polarized light): (a) granodiorite; (b) quartz-diorite; (c) monzogranite; (d) Porphyritic granite.

### 3.1- Granodioritic unit

The widespread granodioritic unit ranges in composition between tonalite to granodiorite and their texture are mostly porphyritic to seriate. It shows medium to coarse-grained textures with a simple mineralogy (Fig. 4a): plagioclase (30–40%), biotite (10–20%), quartz (25–30%) and alkali feldspar (<20%). Apatite, zircon, allanite and opaques are common accessory minerals and some muscovite is present as a secondary mineral. Plagioclase forms rectangular to subhedral plates, 2–3 mm or less in length that exhibit variable amounts of sericitisation. This mineral displays some zoning and, based on the textural relationships, it could be the first felsic mineral to crystallize. Biotite occurs as brown flakes, 2–3 mm in length, with a preferred orientation, but may be kinked due to deformation, and is mostly altered to chlorite and/or titanite, prehnite, muscovite and opaques. Quartz crystals occur as anhedral isolated grains and aggregates which display recrystallisation with undulatory extinction, typical of incipient solid-state deformation.

### 3.2- Quartz-diorite unit

Many small stocks of quartz-dioritic composition are exposed within the granodioritic body. The grain size is not very variable, being 2 mm on average (Fig. 4b). These rocks have a granular to porphyritic texture with plagioclase megacrysts, and are composed predominantly of plagioclase (40–50%), biotite (15–20%), green amphibole (10–15%), quartz (<15%) and alkali feldspar (<5%). Plagioclase occurs as zoned euhedral to subhedral plates, 2–3 mm average size, and sometimes altered to sericite, epidote and calcite. Biotite occurs as brown kinked flakes, 1–3 mm in size, deformed and altered to chlorite, or an aggregate of sphene, prehnite, muscovite, opaques and quartz. Green amphibole forms subhedral to euhedral prismatic crystals, 1–3 mm long, and shows some alteration to biotite, chlorite, epidote and

prehnite. Zircon, titanite and apatite are conspicuous accessory minerals.

### 3.3- Monzogranitic unit

The monzogranitic unit is widely scattered as separate and small outcrops through the Mijan and Hishin area. These rocks are light in colour, fine to coarse-grained, with a granular texture (in the centre of the unit) and a porphyritic texture with feldspar megacrysts at the margin. Mineral assemblages include quartz (30–35%) alkali feldspar (30–35%), plagioclase (25–35%), biotite (5–10%) and some secondary muscovite. Zircon, allanite and apatite are common accessory minerals (Fig. 4c). Quartz intergrowths with K-feldspar and plagioclase form micrographic and/or granophyric textures and myrmekites, respectively. Large phenocrysts of the quartz show undulatory extinction. Perthitic alkali-feldspar occurs as euhedral to subhedral crystals. Plagioclase is commonly zoned and again appears to be the first felsic mineral to crystallize.

### 3.4- Porphyritic granite unit

The porphyritic granite consists of oligoclase and albite (33–35%), microcline (21–25%), quartz (32–40%), biotite (4–8%), and less than 1 percent opaque minerals and texture consists of euhedral to subhedral alkali feldspar and plagioclase megacrysts with fine-grained aplitic groundmass (Fig. 4d). The size and abundance of the megacrysts vary from place to place. Alkali feldspar is typically strongly red-pigmented string perthite and is rarely mantled by plagioclase. The core of plagioclase is strongly altered to sericite and locally to muscovite, epidote, and calcite. The groundmass consists of euhedral, rounded crystals of early quartz (“drop” quartz), euhedral to subhedral plagioclase, subhedral alkali feldspar, and late interstitial quartz. In addition to biotite, accessory minerals include zircon, apatite, fluorite, and ilmenite. These mafic clots may have formed when the early-crystallized phases clustered to minimize their surface

energy (Wall *et al.*, 1987). the porphyritic granite contains abundant miarolitic cavities, pegmatite pockets, and distinct aplitic groundmass having granophyric texture. These textural features are typically associated with high-level granitic intrusions and, in the case of miarolitic cavities, involve separation of a fluid phase. The finegrained aplitic nature can be related to loss of the fluid (undercooling). Miarolitic cavities vary from 0.5 to 2.0 cm in diameter and are usually filled by quartz, plagioclase, alkali feldspar, as well as secondary epidote, chlorite, and kaolinite.

#### 4–Microstructures

According to Laboue (1982), the ‘Medium’ and ‘light’ subfacies were emplaced through a feeder zone. ‘Medium’ and ‘light’ subfacies located in the Mijan area. Then the magma expanded along a NW–SE direction. magma flow and according to which the mylonitic contacts observed in the rims all Intrusive bodies at shearing. Orientations would be coeval and would correspond to the same strain field. The ‘longitudinal’ orientation, developed in the rims of the pluton, is associated with coaxial flow, whereas near the floor and roof contacts of the granites, the ‘oblique’ orientation develops with a non-coaxial strain related to the regional southeastward shearing. Regardless of the emplacement model and related kinematics, the previous studies consider the Mijan area is old caldera and is feeder zone for JBPC (Ghorbani, 2013). It has been suggested that, in this area, the NW–SE-trending large-scale upright folding related to the emplacement and reoriented the primary planar and linear structures of the JBPC. Conversely to the porphyritic granite, very few previous structural works dealt with the leucogranite bodies in the JBPC. However, it is worth noting that the leucogranite Intrusive bodies exhibit a peculiar orientation related to the NW–SE-trending regional extensional strain field. The dominant NW–SE -trending Intrusive bodies, perpendicular to the maximum

extensional direction, might be interpreted as steep-dipping faults open like ‘tension gashes’. Conversely, the NW–SE-trending Intrusive bodies emplaced along NW–SE faults.

It is important to determine which stage of the crystallization and cooling history the fabrics recorded. For example, a magmatic state fabric is acquired when the granite is still above the solidus that is during crystallization, whereas a solid-state fabric characterizes subsolidus conditions. In accordance with several other studies dealing with the microstructures present in granitic rocks (Bouchez *et al.*, 1997; Paterson *et al.*, 1989), the following types of microstructures are defining. The microstructures observed in thin sections from about 200 samples in this study were grouped into three types: (i) magmatic microstructures; (ii) submagmatic microstructures (High temperature microstructures, solid state deformation) and (iii) Mylonitic microstructures (low- temperature, high-stress).

##### 4.1- Magmatic microstructures

Many samples exhibit microstructures that are typical of magmatic flow. However, some signs of a very weak solid-state overprint are sometimes present. They are observed to vary continuously from typically magmatic to incipiently recrystallized. They concern exclusively the granite and granodiorite located in the central of Mijan and less than in the central of Hishin and Korour area. The typically magmatic microstructure is characterized by lath-shaped plagioclase grains with variously sutured to euhedral boundaries, fairly undeformed biotite and amphibole, quartz and K-feldspar as anhedral interstitials in between mainly plagioclase and biotite. Large quartz grains have no more than weak undulose extinction, but frequently present checkerboard patterns of their sub-boundaries (Fig. 5a). They indicate that a small amount of solid-state deformation took place at temperatures close to the granite solidus (Mainprice *et al.*, 1986;

Kruhl, 1996). Intracrystalline fractures in plagioclase with in-fills of residual melt that further crystallized into quartz and minor K-feldspar, attest to the submagmatic state defined by Bouchez *et al.* (1992). The incipiently recrystallized type shows the development of rather large quartz neoblasts (=1 mm) inside or at the rims of larger quartz grains (Fig. 5b). These neoblasts have rather well recovered boundaries indicative of a High temperature overprint. Some kinked biotites and amphiboles, with no compositional changes, point to the

stability of these minerals during incipient High temperature deformation. Some plagioclases also show progressive recrystallization and the observed new grains are polygonised, along with quartz, with equilibrated triple-junction boundaries (Fig. 5c). Myrmekite intergrowths also suggest a rather high temperature process, above 550 °C (Tribe and D'Lemos, 1996). Note that, in the rims of the study area, these microstructures can still be recognized, but are affected by substantial hydrothermal alteration and some superimposed mylonitisation (Fig. 5f).

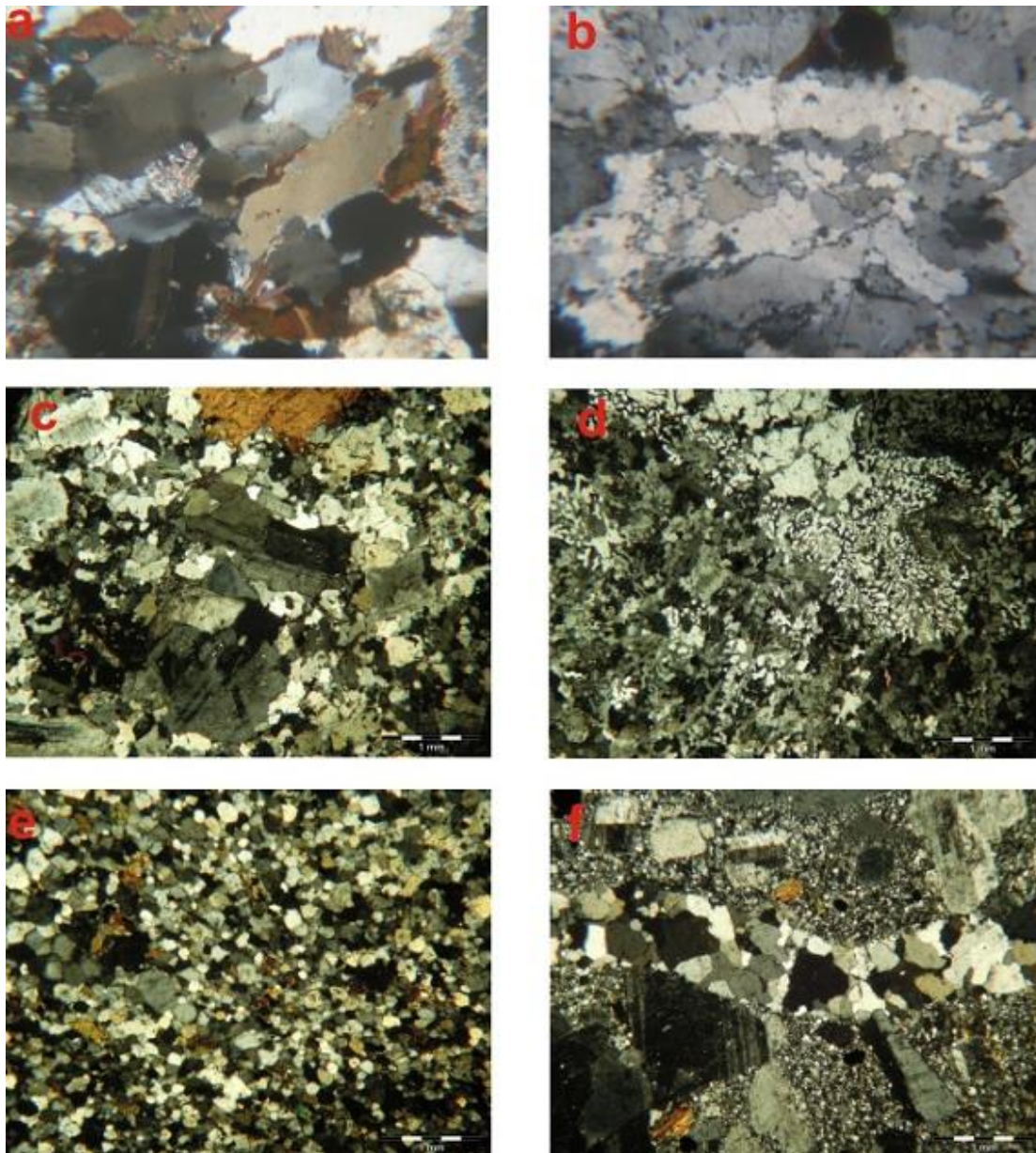


Figure 5) Optical microstructures of the Jebale Barez Plutonic complex. (a) Magmatic: typical checkerboard pattern in quartz; (b) magmatic: development of subgrains in quartz; (c) magmatic: polygonised plagioclase and quartz; (d), submagmatic: Some myrmekites are observed; (e) typically submagmatic: fine-grained, elongate quartz grains; (f) typically mylonitic: pervasive fine-grained quartz surrounding old quartz and plagioclase grains.

#### 4.2- Submagmatic microstructures: high-T, low –stress ( solid state deformation)

Microstructures of this type correspond to a strain imprint, always of a moderate magnitude, that occurred by the end of and/or shortly after the complete crystallization of the magma and observed in Hishin, Korour, and less than in the rim of Mijan area. The typically High temperature microstructures it is marked by a stronger solid-state overprint along with a ubiquitous recrystallization of quartz (Fig. 5d). Hence, only relicts of the primary magmatic microstructure can be recognized. The quartz grains, sometimes elongate, are pervasively replaced by mosaics of new grains of variable sizes indicating their synkinematic recrystallization. Fractures within the feldspars inherited from the magmatic stage, and recrystallization around the plagioclases mantled by neoblasts, are also distinctive features of this microstructure. In the typical High temperature microstructure (Fig. 5e), no original magmatic structure can be recognized. The grain-size is heterogeneous, but generally fine. Quartz grains often form polycrystalline elongate ribbons within a matrix of fractured and partly recrystallized feldspars, as well as recrystallized biotite and amphibole. In addition to, Quartz grains systematically exhibit undulose extinction, often with a chess-board texture, and evidence exists for dynamic recrystallisation, such as lobate grain boundaries. Large quartz grains are rarely observed since they are often replaced by numerous small recrystallised grains with irregular boundaries. biotite is more frequently ‘kinked’ than in the first type of microstructures and some grains are elongated. K-feldspar displays features of intracrystalline deformation, such as undulose extinction. Some myrmekites are also observed. All these criteria are typical of a solid-state deformation (Paterson *et al.*, 1989; Vernon, 2000). As with the magmatic microstructures, these High temperature microstructures can be affected by a

superimposed mylonitisation and/or hydrothermal overprint as described in the next section.

#### 4.3-Mylonitic microstructures: low-T, high-stress (solid-state deformation)

mylonitic character is faint in intensity and is sporadic. Where the previous, underlying microstructure can still be recognized under the microscope without ambiguity. Some micro-shear and fine-grained zones develop in between the larger, primary crystals, and nuclei of recrystallized quartz appear at quartz-grain periphery and sometimes inside quartz grains. It is defined when this mylonitic, high-stress microstructural “landscape” is pervasive (Fig. 4f): very fine-grained matrix of quartz and altered feldspar in between porphyroclasts of mainly quartz and plagioclase; strong undulose extinctions and kinks in quartz. In addition to, ductile deformation is completely lacking in feldspars. Compositional zonings and syneusis of plagioclase are locally observed and K-feldspars show perthitic texture. A few late fractures indicate that a low temperature brittle deformation was recorded in these samples. This is particularly well observed in the Tenaroiieh, Madian, Delfard, Darreh Hamzeh and in the rims all Intrusive bodies located at JBPC. At this stage, all the previous microstructures have disappeared and were replaced by S-C lenticular, more-or-less anastomosed micro-domains. Finally, these mylonitic microstructures are accompanied by the development of hydrothermal mineral phases.

#### 5–Discussion and conclusions

Microscopic observations may be used to separate the primary, magmatic imprint, from the secondary, late- to post-magmatic ones (Guineberteau *et al.*, 1987; Paterson *et al.*, 1989). A magmatic microstructure and crystal shape fabric is usually preserved if no major structural modification of the rock has occurred

following solidification. If kinematic information can be obtained from their fabric, these bodies may be used as markers of crustal deformation at time of their emplacement. New fabrics, due to late deformation, may appear locally in large bodies, or more pervasively in smaller ones. They may modify or erase the earlier fabrics depending on temperature and strain intensity. Magmatic fabrics are always difficult to determine because rock anisotropies are low. The classical measuring procedure is based on time consuming statistics in the field, yielding patterns that are often regarded with little confidence. This is particularly true for the lineation, the most interesting kinematic indicator, which is hard to measure in the field or in the laboratory using the microscope (Bouchez *et al.*, 1983).

Microstructural observations show that samples from JBPC mainly exhibit three kinds of microstructures. On the one hand, purely magmatic to submagmatic deformation microstructures type, which makes 70% of the total, is only observed in the center of the pluton. Among the solid-state deformation microstructures that distribute throughout the rest of the pluton, which followed by brittle deformation after cooling. This feature is typical of syntectonic intrusions. The syntectonic plutons might reflect different kinds of fabrics responding in part to the internal forces and partly to the regional kinematics during cooling and solidification of magma (Hutton, 1982). The good agreement of magmatic and solid-state foliations suggests that the tectonic forces responsible for generating the magmatic fabric in the pluton continued to influence these rocks during/after crystallization. This nature and the continuous passage from magmatic to solid-state deformation have been suggested to result from deformation of pluton as they crystallize by tectonic shortening (Castro, 1990), granitoids that intruded active shear zones (Guineberteau *et al.*, 1987), or simply from the ascent of a diapir with a solid external carapace (Cruden

1990). The mylonitic to submylonitic microstructures clearly cluster in rims, WNW–ESE striking corridor that crosscuts the whole pluton. Although those subsolidus structures record the deformation after the full crystallization of the magma, this deformation is considered as a continuum with respect to the one occurring during the purely magmatic stage, since no later regional deformation occurs. However, this fabric may be due either to internal dynamics of the magma body or to a regional strain field. The similarity between regional extensional and thermal aureole structures shows that minerals formed during contact metamorphism, that is during pluton emplacement and crystallization, underwent the regional extensional tectonic event. Although microscopic observations do not show a significant amount of stretching in granite samples, the occurrence of E-trending elongated enclaves and N–S-trending leucogranitic dykes considered as cross-joints, i.e. perpendicular to maximum incremental stretching direction (Faure *et al.*, 1992), indicates that the NW–SE-trending elongation is probably also recorded in the granite.

Field observations, Major structural and morphologic elements suggested that Mijan area is old caldera. We can observe some of body of caldera in the Mijan area include: topographic rim, inner topographic wall, bounding faults, structural caldera floor, intracaldera fill (mainly ponded ash-flow tuff and landslide debris from caldera walls), and the underlying magma chamber or solidified pluton (Lipman, 1984). The topographic rim is simply the escarpment that bounds the subsided area of a caldera, beyond which lie largely undisturbed outer volcanic slopes. The rim encloses both the subsided area and also the area of scarp retreat due to rock falls and mass wasting. Arcuate bounding faults (ring faults) are exposed at some deeply eroded calderas (mainly 5 km and greater in diameter), unambiguously defining plate (piston) subsidence, for instance, Bennett

Lake in Canada (Lambert, 1974), Lake City and Silverton in the western San Juan Mountains (Lipman, 1976), Grizzly Peak in central Colorado (Fridrich *et al.*, 1991), and many volcanic “cauldrons” and plutonic ring complexes in older terranes (summarized in Smith and Bailey, 1968; Williams and McBirney, 1979; Lipman, 1984). Presence of bounding ring faults in some less eroded calderas can be inferred from the distribution of postcollapse vents, symmetrical resurgent uplift of caldera-filling volcanic rocks, and evidence for vents of the caldera-forming eruption along arcuate segments of caldera margins (Smith and Bailey, 1968; Bacon, 1983; Hildreth and Mahood, 1986). Ring faults that dip steeply inward at shallow crustal levels may steepen with depth and dip outward at levels just above the magma chamber into which the caldera subsided (Williams, 1941; Branney, 1995). Magma chambers, preserved as solidified plutons or batholiths, are exposed in many

deeply eroded ash-flow calderas, as indicated by petrologic and age correlations with erupted volcanics. Such plutons have commonly been emplaced within a few kilometers of the regional volcanic surface, their roof zones protruding into the syneruptive fill of the associated caldera summarized in Lipman, 1984). Accumulation of silicic low-density magma in a large shallow chamber, which can generate uplift and tensile stresses at the surface, could be important in initiating ring faulting and permitting caldera collapse (Gudmundsson, 1988; Marti *et al.*, 1994). Such tumescence associated with growth of a subvolcanic magma chamber, which has been recorded instrumentally during many monitored eruptions and episodes of volcanic unrest, may be inadequate in magnitude to generate geologic structures that are detectable for prehistoric activity. Shallow depths to incompletely solidified caldera-related magma chambers are documented for a few active calderas.

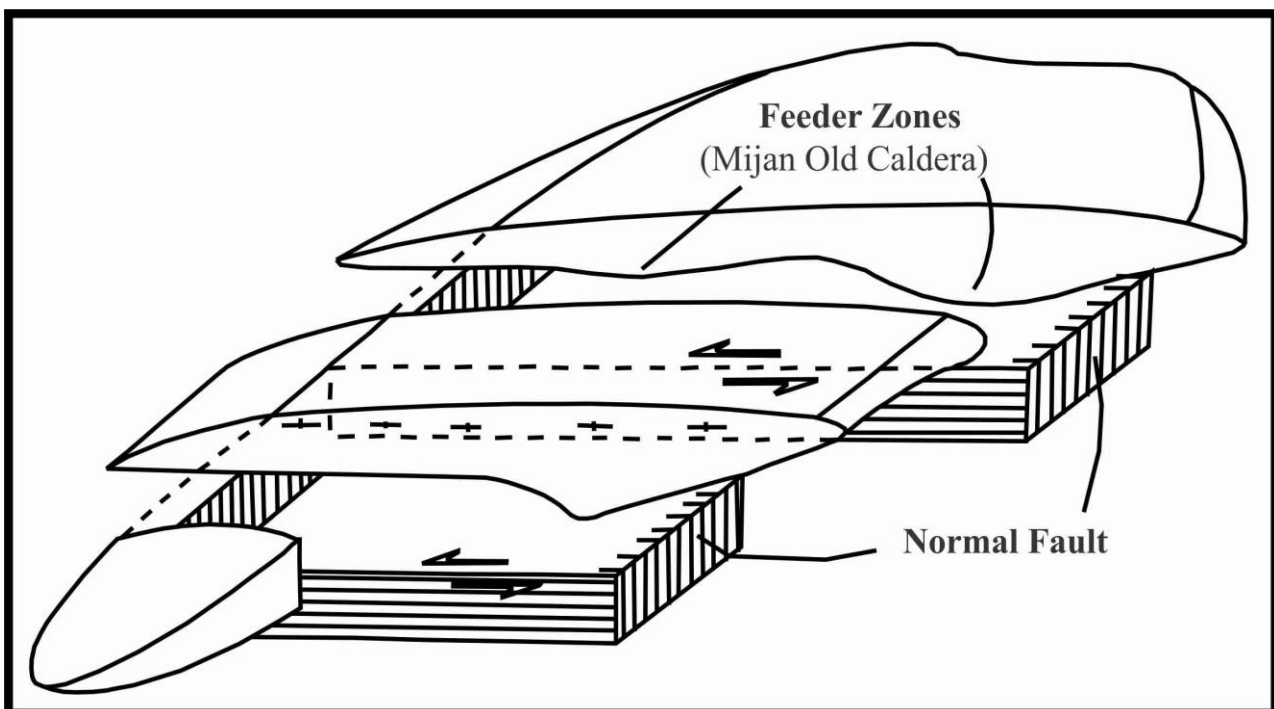


Figure 6) Emplacement Model for Jebale Barez Plutonic complex. Mijan Old Caldera is feeder zone and magma has been intrusion. Magma has been percolated through Mijan caldera and emplacement Forms of Sill along the shear zone during various periods.

Seismic-attenuation studies, magnetic curietemperature depths, and other geophysical data indicate presence of magma at depths as shallow as 4–7 km at the 0.7-Ma Long Valley

caldera in eastern California (Sanders, 1984; Ponko and Sanders, 1994; Steck and Prothero, 1994; Sanders *et al.*, 1995). At several calderas high-resolution dating has documented cooling

of subcaldera plutons within brief time intervals after caldera subsidence, at the Chegem caldera in southern Russia,  $^{40}\text{Ar}/^{39}\text{Ar}$  mineral ages for eight samples of thin outflow tuff, thick intracaldera tuff, and intracaldera resurgent intrusion of porphyritic granodiorite are analytically indistinguishable at 2.82B0.02 Ma (Gazis *et al.*, 1995). Several recent studies have inferred important roles for sills of fine-grained hypabyssal rocks during caldera collapse (Gudmundsson, 1988) and resurgence (Fridrich *et al.*, 1991; du Bray and Pallister, 1991), including introducing a special category of “laccocaldera” (Henry and Price, 1989). Other deeply eroded calderas expose large steep-sided subcaldera plutons containing granitic textures transitional to typical mesozonal batholithic bodies (Lipman, 1984; Takahashi, 1986; Johnson *et al.*, 1989; Lipman *et al.*, 1993; John, 1994; Fiske and Tobisch, 1994).

Evidence below suggested that Magma emplacement Sill form in the JBPC. The term sill is synonymous with concordant intrusive sheet. This means that the sill does not cut across preexisting rocks, in contrast to dikes, discordant intrusive sheets which do cut across older rocks. Sill is fed by dikes, except in unusual locations where they form in nearly vertical beds attached directly to a magma chamber. These planes or weakened areas allow the intrusion of a thin sheet-like body of magma paralleling the existing bedding planes, concordant fracture zone, or foliations. Sill parallel beds (layers) and foliations in the surrounding country rock. They can be originally emplaced in a horizontal orientation, although tectonic processes may cause subsequent rotation of horizontal sill into near vertical orientations. Intruded sills will show partial melting and incorporation of the surrounding country rock. On both contact surfaces of the country rock into which the sill has intruded, evidence of heating will be observed. Sill generally form at shallow depths (up to many kilometers) below the surface, the

pressure of overlying rock prevents this from happening much, if at all. All these properties are in JBPC. Perhaps resurgent intrusions initially spread as sill-like bodies near the base of the caldera fill, developing into stock-like plutons as continued emplacement of intrusive material gravitationally loads caldera-floor rocks and encourages block stoping, as proposed by Hon and Fridrich (1989). Therefore we can be assumed that the whole JBPC is located in shear zone. Mijan Old Caldera is feeder zone and magma has been intrusion. Magma has been percolated through Mijan caldera and emplacement Forms of Sill along the shear zone during various periods (Fig. 6). Furthermore, the present concordance of metamorphic foliations and solid state fabrics suggests that the tectonic regime was active late in the evolution of the complex. Transpression regime which demonstrated by most of these structures and features is the best tectonic model for the emplacement of JBPC.

#### **Acknowledgments:**

The authors would like to thank Dr. E. Elahpour, and an anonymous reviewer for their appreciate comments which help us to improve manuscript.

#### **References:**

- Amidi, M., Majidi, B. 1977. Geological map of Hamaedan 1:250,000, Geological Survey of Iran.
- Bacon, C.R. 1983. Eruptive history of Mount Mazama and Crater Lake caldera, Cascade Range, USA. *Journal of Volcanology and Geothermal Research*: 18, 57–115.
- Berberian, F., Berberian, M. 1981. Tectono-plutonic episodes in Iran, In: Zagros, Hindu Kush and Himalaya Geodynamic Evolution. American Geophysical Union, Geodynamic Series: 3, 5–32.
- Bucher, K., Frey, M. 1994. Petrogenesis of metamorphic rocks. Springer-Verlag, Berlin Heidelberg New York.

- Bouchez, J.L., Lister, G.S., Nicolas, A. 1983. Fabric asymmetry and shear sense in movement zones. *Geologische Rundschau*: 72, 401–419.
- Bouchez, J.L., Delas, C., Gleizes, G., Nedelec, A., Cuney, M. 1992. Submagmatic microfractures in granites. *Geology*: 20, 35–38.
- Bouchez, J.L. 1997. Granite is never isotropic: an introduction to AMS studies of granitic rocks. In: Bouchez, J.-L., Hutton, D.H.W., Stephens, W.E. (Eds.), *Granite: From Segregation of Melt to Emplacement Fabrics*. Kluwer Academic Publishers, Dordrecht, pp. 95–112.
- Branney, M.J. 1995. Downsag and extension at calderas. New perspectives on collapse geometries from ice-melt, mining, and volcanic subsidence. *Bulletin of Volcanology*: 57, 303–318.
- Caillet, C., Dehlavi, P., Martel-Jantin, B. 1978. Géologie de la région de Saveh (Iran) Contribution a l'étude du volcanisme et du plutonisme Tertiaires de la zone de l'Iran Central: Thèse 3 ème cycle. Univ. Grénoble, France, 325pp.
- Castro, A., de la Rosa J.D., Stephens W.E. 1990. Magma mixing in the subvolcanic environment: petrology of the Gerena interaction zone near Seville, Spain. *Contributions to Mineralogy and Petrology*: 105, 9–26.
- Cruden, A.R., Tobisch, O.T., Launeau, P. 1999. Magmatic fabric evidence for conduit-fed emplacement of a tabular intrusion: Dinkey Creek Pluton, central Sierra Nevada batholith, California. *Journal of Geophysical Research*: 104, 10511–10530.
- Darvishzadeh, A. 2005. *Geology of Iran*, Amirkabir Publication, Tehran (in Persian).
- Dimitrijevic, M.D. 1973. *Geology of Kerman region*. Geological Survey of Iran: Report 52, 334 p.
- Du Bray, E. A., Pallister, J. S. 1994. Geologic map of the Chiricahua Peak quadrangle Cochise County, Arizona. US Geological Survey, Geological Quadrangle Map GQ-1733.
- Emami, M.H. 1981. Géologie de la région de Qom-Aran (Iran): Contribution a l'étude dynamique et géochimique du volcanisme Tertiaire de l'Iran Central: Ph.D., Thèse, Univ., Grenoble, France, 489p.
- Faure, M., Pons, J., Babinault, J.F. 1992. Le pluton du Pont-de-Montvert: un granite syntectonique extravasé vers l'Est pendant le désépaississement crustal varisque du Massif Central français. *Comptes Rendus de l'Académie des Sciences*: 315, 201–208.
- Fridrich, C. J., Smith, R. P., DeWitt, E., McKee E. H. 1991. Structural, eruptive, and intrusive evolution of the Grizzly Peak caldera, Sawatch Range, Colorado. *Geological Society of America Bulletin*: 103, 1160–1177.
- Fiske, R. L., Tobisch, O. T. 1994. Middle Cretaceous ash-flow tuff and caldera-collapse deposit in the Minarets caldera, east-central Sierra Nevada, California. *Geological Society of America Bulletin*: 106, 582–593.
- Gazis, C. A., Lanphere, M. A., Taylor, H. P. Jr., Gurbanov, A. 1995.  $^{40}\text{Ar}/^{39}\text{Ar}$  and  $^{18}\text{O}/^{16}\text{O}$  studies of the Chegem ash-flow caldera and Eldjurta Granite: cooling of two late Pliocene igneous bodies in the Greater Caucasus Mountains, Russia. *earth and planetary science letters*: 134, 377–391.
- Ghorbani, M. 2013. *Magmatism and Metamorphism of Iran*. Lecture notes, School of Earth Sciences, Shahid Beheshti University, Tehran, Iran, (in Persian).
- Gudmundsson, A. 1988. Formation of collapse calderas. *Geology*: 16, 808–810.
- Guineberteau, B., Bouchez, J.L., Vigneresse, J. L. 1987. The Mortagne granite pluton (France) emplaced by pull-apart along a

- shear zone: structural and gravimetric arguments and regional implication. *Geological Society of America Bulletin*: 99, 763–770.
- Hassanzadeh, J. 1993. Metallogenic and tectono-magmatic events in the SE sector of the Cenozoic active continental margin of Iran (Shahr e Babak area, Kerman province). Unpublished Ph.D. thesis, University of California, Los Angeles, 204 p.
- Heilbronner, R. 2000. Optical orientation imaging. In: Jessell, M. W., Urai, J. L. (eds) *Stress, strain and structure, a volume in honour of W.D. Means*. *J Virt Explorer* 2.
- Hildreth, W., Mahood, G. A. 1986. Ring-fracture eruption of the Bishop Tuff. *Geological Society of America Bulletin*: 97, 396–403.
- Henry, C. D., Price, J. G. 1989. The Christmas Mountains caldera complex, Trans-Pecos Texas: the geology and development of a laccocaldera. *Bulletin of Volcanology*: 52, 97–112.
- Hon, K., Fridrich, C. 1989. How calderas resurge. in *IAVCEI Abstracts: New Mexico Bureau of Mines and Mineral Resources Bulletin*: 131, p 135.
- Hutton, D. H. W. 1982. A tectonic model for the emplacement of the Main Donegal granite, NW Ireland. *Journal of the Geological Society London*: 139, 615–631.
- John, D. A. 1994. Tilted middle Tertiary ash-flow calderas and subjacent granitic plutons, southern Stillwater Range, Nevada. Cross sections of an Oligocene igneous center. *Geological Society of America Bulletin*: 107, 180–200.
- Johnson, C. M., Shannon, J. R., Fridrich, C. J. 1989. Roots of ignimbrite calderas: batholithic plutonism, volcanism, and mineralization in the southern Rocky Mountains, Colorado and New Mexico. *Bureau of Mines and Mineral Resources Memoir*: 46, 275–302.
- Laboue, M. 1982. Etude structurale du massif de la Margeride. PhD thesis, Université de Clermont-Ferrand, 140p.
- Lambert, M. B. 1974. The Bennett Lake cauldron subsidence complex, British Columbia and Yukon Territory. *Geological Survey of Canada Bulletin*: 227, 1–213.
- Lipman, P. W. 1976. Caldera collapse breccias in the western San Juan Mountains, Colorado. *Geological Society of America Bulletin*: 87, 1397–1410.
- Lipman, P. W. 1984. The roots of ash-flow calderas in North America: windows into the tops of granitic batholiths. *Journal of Geophysical Research*: 89, 8801–8841.
- Lipman, P. W., Bogatikov, O. A., Tsvetkov, A. A., Gazis, C., Gurbanov, A. G., Hon, K., Koronovsky, N. V., Kovalenko, V. I., Marchev, P. 1993. 2.8-Ma ash-flow caldera at Chegem River in the northern Caucasus Mountains (Russia), contemporaneous granites, and associated ore deposits. *Journal of Volcanology and Geothermal Research*: 57, 85–124.
- Kruhl, J.H. 1996. Prism- and basal-plane parallel subgrain boundaries in quartz: a microstructural geothermobarometer. *Journal of Metamorphic Geology*: 14, 581–589.
- Mainprice, D., Bouchez, J.L., Blumenfeld, P., Tubia, J.M. 1986. Dominant c-slip in naturally deformed quartz: implications for drastic plastic softening at high temperature. *Geology*: 14, 819–822.
- Mainprice, D., Popp, T., Gueguen, Y., Huenges E., Rutter, E. H., Wenk, H. R., Burlini, L. 2003. Physical properties of rocks and other geomaterials, a special volume to honour professor H. Kern. *Tectonophysics*: 370, 1–311.

- Marti, J., Ablay, G. J., Redshaw, L. T., Sparks R. S. J. 1994. Experimental studies of collapse calderas. *Journal of the Geological Society London*: 151, 919–929.
- McLaren, A. C., Pryer, L. L. 2001. Microstructural investigation of the interaction and interdependence of cataclastic and plastic mechanisms in feldspar crystals deformed in the semi-brittle field. *Tectonophysics*: 335, 1–15.
- Moine-Vaziri, H. 1985. *Volcanisme tertiaire et quaternaire en Iran*: These d'Etat. Univers. Paris-Sud, Orsay.
- Passchier, C. W. 1982a. Mylonitic deformation in the Saint-Barthélemy Massif, French Pyrenees, with emphasis on the genetic relationship between ultramylonite and pseudotachylyte. (Ph.D. Thesis). *GUA Papers of Geology*: 16, 1–173.
- Passchier, C. W. 1982b. Pseudotachylyte and the development of ultramylonite bands in the Saint-Barthélemy Massif, French Pyrenees. *Journal of Structural Geology*: 4, 69–79.
- Passchier, C. W., Trouw, R. A. J., Ribeiro, A., Paciulo, F. 2002. Tectonic evolution of the southern Kaoko Belt, Namibia. *Journal of African Earth Sciences*: 35, 61–75.
- Paterson, S. R., Vernon, R. H., Tobisch, O. T. 1989. A review of criteria for the identification of magmatic and tectonic foliations in granitoids. *Journal of Structural Geology*: 11, 349–364.
- Ponko, S. C., Sanders, C. O. 1994. Inversion for P and S wave attenuation structure, Long Valley caldera, California. *Journal of Geophysical Research*: 99, 2619–2635.
- Ramsay, J. G. 1967. *Folding and fracturing of rocks*. McGraw Hill, New York.
- Sabzehei, M. 1994. Geological Quadrangle Map of Iran, No. 12, Hajiabad, 1:250,000, First compilation by Berberian, M., final compilation and revision by Sabzehei, M., Geological Survey of Iran.
- Sanders, C. O. 1984. Location and configuration of magma bodies beneath Long Valley, California, determined from anomalous earthquake signals. *Journal of Geophysical Research*: 89, 8287–8302.
- Sanders, C. O., Ponko, S. C., Nixon, L. D., Schwartz, E. A. 1995. Seismological evidence for magmatic and hydrothermal structure in Long Valley caldera from local earthquake attenuation and velocity tomography. *Journal of Geophysical Research*: 100, 8311–8326.
- Simpson, C. 1985. Deformation of granitic rocks across the brittle-ductile transition. *Journal of Structural Geology*: 7, 503–511.
- Shafiei, B., Haschke, M., Shahabpour, J. 2009. Recycling of orogenic arc crust triggers porphyry Cu mineralization in Kerman Cenozoic arc rocks, southeastern Iran. *Mineralium Deposita*: 44, 265–283.
- Smith, R. L., Bailey, R. A. 1968. Resurgent cauldrons. *Geological Society of America Memoirs* 116:83–104. Spry, A.: 1969, *Metamorphic textures*, Pergamon, London, 350p.
- Steck, L. K., Prothero, W. A. 1994. Crustal structure beneath Long Valley caldera from modeling of teleseismic P wave polarizations and Ps converted waves. *Journal of Geophysical Research*: 99, 6881–6898.
- Takahashi, M. 1986. Anatomy of a Middle Miocene Valles-type caldera cluster. Geology of the Okueyama volcano-plutonic complex, southwest Japan. *Journal of Volcanology and Geothermal Research*: 29, 33–70.
- Takin, M. 1972. Iranian geology and continental drift in the Middle East. *Nature*: 235, 147–150.

- Trčková, J., Šrein, V., Šťastný, M., Živor, R. 2008. The relationship between gneisses from the Kola superdeep borehole and their surface analogues. *Acta Geodynamica et Geomaterialia*: 5, 57–63.
- Tribe, I.R., D’Lemos, R. S. 1996. Significance of a hiatus in down-temperature fabric development within syntectonic quartz diorite complexes, Channel Islands, UK. *J. Geol. Soc. Lond.* 153 (1), 127–138.
- Vernon, R. H. 1989. Porphyroblast-matrix microstructural relationships recent approaches and problems. In: Daly JS, Cliff RA, Yardley BWD (eds) *Evolution of metamorphic belts*. *Journal of the Geological Society London, Special Publication*: 43, 83–102.
- Vernon, R. H., Collins, W. J., Paterson, S. R. 1993a. Pre-foliation metamorphism in lowpressure/hightemperatureterrains. *Tectono physics*: 219, 241–256.
- Vernon, R. H. 2000. Review of microstructural evidence of magmatic and solid-state flow. *Electronic Geosciences*: 5:2.
- Williams, H. 1941. Calderas and their origin. *Bulletin of the Department of Geological Sciences*: 25, 239–346.
- Williams, H., McBirney, A. R. 1979. *Volcanology*. Freeman, Cooper and Co, San Francisco.